Contents available at **PubMed**
www.clinicalandtranslationalinvestigation.com

Rev Invest Clin. 2024;76(4):173-84 ORIGINAL ARTICLE

Curzerene Suppresses Hepatocellular Carcinoma Progression Through the PI3K/AKT/MTOR Pathway

Yihui Luo[1], Zhenchang Wang[1]*, Jun'e Jiang[1], Shanshan Wu[1], and Yang Zhai[2]

Departments of [1]Spleen and Stomach Liver Disease and[2] International Medicine, Guangxi International Zhuang Medicine Hospital, Guangxi, China

ABSTRACT

Background: Hepatocellular carcinoma (HCC) is one of the most aggressive cancers worldwide. Curzerene is a sesquiterpene and component of *Curcuma* rhizomes and has anti-tumor and anti-inflammatory properties. **Objective:** The study aimed to investigate the effects of curzerene on the malignant phenotypes and tumor growth in HCC. **Methods:** Various concentrations of curzerene were used to treat human HCC cells (Huh7 and HCCLM3). Cell viability, apoptosis, cell cycle, invasion, and migration were detected by 3-(4,5-Dimethylthiazol-2-yl)-2,5-diphenyltetrazolium bromide, flow cytometry, Transwell, and wound healing assays. Cell cycle-, apoptosis-, and signaling pathway-related proteins were analyzed by Western blot analysis. A mouse xenograft model was established to analyze the anti-tumor effects of curzerene *in vivo*. **Results:** Curzerene repressed the proliferation, invasion, and migration of Huh7 and HCCLM3 cells. Curzerene also induced G2/M cycle arrest and cell apoptosis. Curzerene downregulated the CDK1, cyclin B1, PCNA, Bcl-2, matrix metallopeptidases (MMP)2, and MMP9 protein expression and upregulated the Bax, cleaved caspase3, and cleaved poly ADPribose polymerase protein expression in HCC cells. Curzerene restrained the phosphorylation of PI3K, AKT, and the Mammalian target of rapamycin (mTOR) in Huh7 and HCCLM3 cells. The *in vivo* data revealed that curzerene inhibited HCC tumor growth and decreased the expression of phosphorylated mTOR in xenograft mouse models. **Conclusion:** Curzerene inhibited cell malignancy in vitro and tumor growth in vivo in HCC, suggesting that curzerene may be a candidate agent for anti-HCC therapy. (REV INVEST CLIN. 2024;76(4):173-84)

Keywords: Hepatocellular carcinoma. Curzerene. Cell cycle. MMP9. mTOR.

INTRODUCTION

Hepatocellular carcinoma (HCC) is a highly aggressive malignancy and the main cause of cancer-related mortality worldwide[1,2]. Epidemiological data show that the pre-disposing factors for HCC include smoking[3], alcohol consumption[4], type 2 diabetes[4], aflatoxin exposure[5], and hepatitis virus infection[6]. To date, liver transplantation and surgical resection are the main therapeutic strategies for HCC[7]. Although substantial progress has been achieved in HCC diagnosis and treatment, patients with HCC still suffer from metastasis and local invasion, leading to poor overall survival[8,9]. Therefore, there is a need to systematically investigate the mechanisms underlying HCC development.

***Corresponding author:**
Zhenchang Wang
E-mail: wangzhenchang924@hotmail.com

Received for publication: 24-01-2024
Approved for publication: 17-04-2024
DOI: 10.24875/RIC.24000018

Chemotherapy is an important treatment modality for advanced HCC. It can destroy tumor cells but inevitably produces serious side effects[10]. Recently, scholars have been committed to studying the active ingredients of traditional Chinese medicine with anticancer effects and low toxicity[11]. *Curcuma longa* is a traditional Chinese medicine, and its extracts have been applied for the treatment of human cancers and eye diseases[12]. Curzerene ($C_{15}H_{20}O$; Fig. 1A) is an active component of *C. longa* and has shown antitumor efficacy. In glioblastoma, curzerene restrains cell migration and invasion and induces cell apoptosis. Meanwhile, it represses tumor growth *in vivo* and simultaneously prolongs the survival time of tumor-bearing nude mice[13]. In addition, curzerene reduces Glutathione S-transferase A1 expression in lung cancer and exhibits low toxicity to the major organs of mice[14]. However, the biological functions of curzerene in HCC remain unknown.

The mammalian target of rapamycin (mTOR) is a member of the PI3K-related protein kinase family[15]. The PI3K/AKT/mTOR signaling pathway is frequently activated in various cancers and regulates cell metabolism and growth[16]. Previous studies have reported the essential roles of this pathway in the invasion, migration, survival, and proliferation of tumor cells[17,18]. The suppressive effects of curzerene on the mTOR pathway have been validated in glioma cells[19]. Nonetheless, whether curzerene can modulate the PI3K/AKT/mTOR pathway in HCC, it remains unknown.

In this study, we explored the effects of curzerene on HCC cell growth and investigated its related mechanisms. We hypothesized that curzerene can inhibit HCC progression. This study may help to identify novel drug candidates for HCC treatment.

METHODS

Cell culture

Human HCC cells (Huh7 and HCCLM3) and human normal hepatocytes (L-02) were commercially obtained from Oricell (Shanghai, China) and cultured in Dulbecco's modified Eagle's medium (M0100, WHELAB, Shanghai) supplemented with 10% FBS (76294-180, AVANTOR, Australia) and 100 µg/mL streptomycin/penicillin (Beyotime) at 37°C with 5% CO_2.

Cell treatment

For curzerene treatments, Huh7, HCCLM3, and L-02 cells were seeded in 96-well plates and treated with curzerene (12.5, 25, 50, 100, and 200 µM) for 24 h. Purified curzerene (HPLC≥98%; wkq-00193) was purchased from Weikeqi Biotechnology (Sichuan, China).

3-(4,5-Dimethylthiazol-2-yl)-2,5-diphenyltetrazolium bromide (MTT) assay

Huh7, HCCLM3, and L-02 cells (5000 cells/well) were plated in 96-well plates. The next day, the cells were treated with curzerene for 24 h. After incubation, 20 µL of MTT solution (PH0533; Phygene, Fuzhou, China) were added and incubated for 4 h at 37°C. Then, 150 µL of DMSO were added to the wells to dissolve the formazan. The optical density value was detected using a microplate reader at 570 nm. Each experiment was repeated 5 times.

Colony formation assay

Huh7 and HCCLM3 cells were seeded in 6-well plates (10,000 cells/well). The cells were treated with curzerene and incubated for 14 days. The colonies were fixed with 4% paraformaldehyde for 30 min and stained with 0.6% Giemsa stain (LM8M013; LMAI Bio, Shanghai) for 30 min. The colonies were counted using ImageJ (version 1.49v). Each experiment was repeated 5 times.

Flow cytometry analysis

For cell cycle evaluation, Huh7 and HCCLM3 cells were seeded in 6-cm culture dishes and treated with concentrations of curzerene for 24 h. Cells were then fixed in 70% cold ethanol for 1 h at −20°C. Cells were resuspended in 500 µL of PBS and stained with PI/RNase Staining Buffer (HY-000525; BD Biosciences) according to the manufacturer's instructions. After incubation for 15 min, cell cycle analysis was performed using a FACScan flow cytometer (CA, USA). For cell apoptosis evaluation, HCC cells were prepared into a suspension and seeded in 6-well plates (2×10^5 cells/mL). After incubation with curzerene for 24 h, the cells were stained as per the instructions for the Apoptosis Detection Kit (MX3210; Maokang Biotech) and subsequently subjected to flow cytometry analysis. All the data in flow cytometry were analyzed by CXP Software (Beckman Coulter, CA). Each experiment was repeated 5 times.

Figure 1. Curzerene inhibited the growth of HCC cells. **A:** chemical structure of curzerene. **B:** human HCC cells (Huh7 and HCCLM3) and human normal hepatocytes (L-02) were treated with various concentrations of curzerene for 24 h, followed by measurement of cell viability using MTT assay. Measurement data are expressed as mean ± SD. n = 5. *p < 0.05; ***p < 0.001.

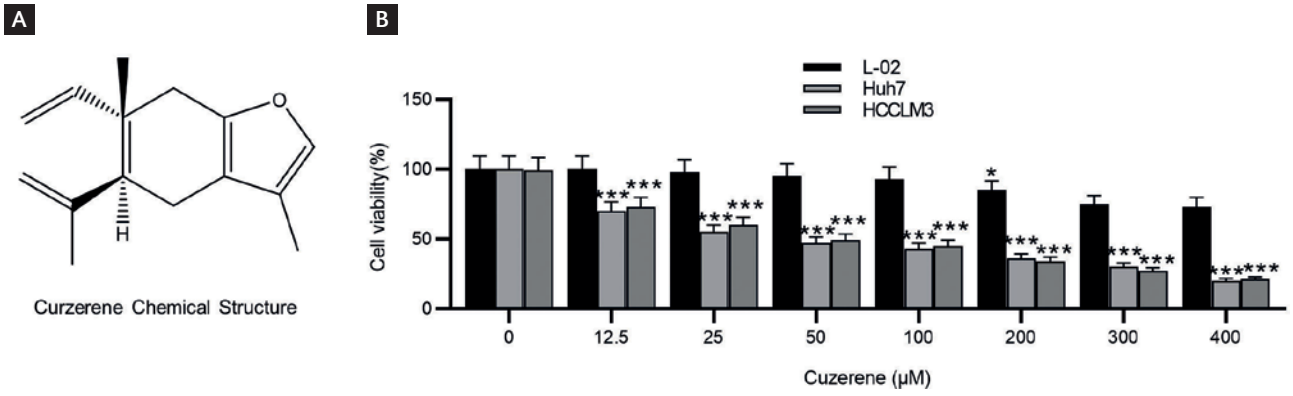

Wound healing assay

Huh7 and HCCLM3 cells were cultured in 6-well plates at 4×10^5 cells/well. After reaching about 90% confluence, cells were scratched using a 200 μL pipette tip (CN-24502-23; Cole-Parmer Instrument, Shanghai). Cell debris was washed away, and the medium was replaced with 1 mL of serum-free culture medium. Images were captured with a digital microscope at 0 h and 24 h, respectively. The wound width was analyzed using ImageJ. Each experiment was repeated 5 times.

Transwell assay

Matrigel (50 μL; Corning, CA) diluted in serum-free medium was added to the upper chamber of a Transwell apparatus for 1 h. After gel solidification, the digested cells were suspended in a serum-free medium. A cell suspension (200 μL) was added to the upper chamber. A complete medium containing 20% FBS was added to the lower chamber. After 24 h, the cells on the upper surface were removed with a cotton ball. The invaded cells were stained with 0.1% crystal violet for 30 min. Finally, the cells were photographed and counted under an inverted microscope. Each experiment was repeated 5 times.

Immunoblotting analysis

Protein extraction and Western blotting were performed as previously described[20]. Western blotting was performed using primary antibodies, including CDK1 (ab265590, 1:1,000), cyclin B1 (ab181593, 1:2,000), PCNA (ab92552, 1:3,000), matrix metallopeptidases (MMP)2 (ab92536, 1:2,000), MMP9 (ab76003, 1:3,000), Bax (ab182734, 1:1,000), Bcl-2 (ab182858, 1:2,000), cleaved caspase3 (ab32042, 1:500) (ab214430, 1:5,000), cleaved Poly ADPribose polymerase (PARP) (AF7023, 1:1,000) (AF5240, 1:1,000), PI3K (AF6241, 1:2,000), p-PI3K (AF3242, 1:2,000), mTOR (AF6308, 1:2,000), p-mTOR (AF3308, 1:2,000), AKT (AF6261, 1:2,000), p-AKT (AF0016, 1:2,000), and GAPDH (AF7021, 1:3,000). Protein bands were developed with an ECL Plus kit (P0018; Beyotime, Shanghai). ImageJ software (version 1.49v) was used to analyze the gray value. Each experiment was repeated 5 times.

In vivo experiments

Previous studies reported that both female and male mice can be used in xenograft tumor models of HCC (Ma, 2019 #7909) (Yan, 2021 #7908) (Yan, 2021 #7908). Female mice are generally docile. To exclude the impact of gender, we only used female mice here. BALB/c nude mice (female, aged 4 weeks, 10-17 g) were commercially obtained from Cavens Laboratory Animal Co., Ltd. (Changzhou, China) and maintained in a pathogen-free animal laboratory. All experimental procedures were performed following the guidelines for laboratory animal use set by the National Institutes of Health and approved by the Institutional Animal Care and Use Committee of Guangxi International Zhuang Medicine Hospital. The armpit of each

nude mouse was subcutaneously injected with 1×10^6 Huh7 cells. After tumor formation for 7 days, curzerene was intraperitoneally injected into mice every other day at a dose of 6×10^{-4} mol/kg[14]. The mice in the control groups only received an equal volume of normal saline. Tumor volume was calculated every 3 days. After drug injection for 25 days, tumors were collected and weighed.

Immunofluorescence staining

The harvested tumor tissues (4 μm thick) were blocked with 5% bovine serum albumin for 1 h and incubated with primary antibodies against p-mTOR (AF3308, 1:100) and anti-Ki67 (AF0198, 1:100) at 4°C overnight. The fluorescence signals were captured with a fluorescence microscope (Olympus BX53, Tokyo, Japan). Each experiment was repeated 4 times.

TUNEL staining

Following the protocols of the TUNEL apoptosis kit (CSK00001; Chemstan, Wuhan, China), the tumor sections were dewaxed, hydrated, washed, and then treated with 20 μg/mL Protease K solution (ST523, Beyotime, Shanghai) at 37°C for 15 min. The slices were washed 3 times and incubated with 50 μL of TUNEL solution for 1 h in the dark. After staining with DAPI, apoptosis was observed by fluorescence microscopy. Each experiment was repeated 4 times.

Statistical analysis

Experimental data are shown as the mean ± standard deviation (SD) and were analyzed using SPSS 21.0 software. The difference between two groups was compared using the student's t-test, while that among multiple groups using a one-way analysis of variance. $p < 00.05$ was considered statistically significant.

RESULTS

Curzerene inhibited the growth of hepatocellular carcinoma cells

The cytotoxic effects of curzerene (Fig. 1A) on HCC cells were examined. Human HCC cells (Huh7 and HCCLM3) and human normal hepatocytes (L-02) were incubated with curzerene for 24 h. As MTT assays demonstrated, the proliferation of Huh7 and HCCLM3 cells was restrained by curzerene in a dose-dependent manner (Fig. 1B). The IC_{50} values for Huh7 and HCCLM3 at 24 h were 47 ± 4.36 μM and 49 ± 4.45 μM, respectively. The viability of L-02 cells was decreased by approximately 15% when the concentration of curzerene was 200 μM (Fig. 1B), indicating that curzerene has low toxicity to normal liver cells. Similarly, Huh7 and HCCLM3 cells treated with curzerene (10, 20, and 40 μM) exhibited reduced colony formation compared to untreated cells (Fig. 2A and B). Here, the impact of curzerene on the cell cycle in Huh7 and HCCLM3 cells was determined. Huh7 and HCCLM3 cells were incubated with 10, 20, and 40 μM curzerene, respectively, for 24 h, and the cell cycle-related proteins were analyzed. We found that, in HCC cells, the CDK1, cyclin B1, and PCNA protein levels were reduced after curzerene treatment (Fig. 2C and D). Furthermore, the proportion of cells in the G2/M phase was increased after curzerene treatment (Fig. 2E and F), suggesting that curzerene restrains HCC cell growth by inducing G2/M cycle arrest.

Curzerene suppressed the motility of hepatocellular carcinoma cells

As shown in Fig. 3A and B, 20 and 40 μM curzerene notably restrained the wound healing in Huh7 and HCCLM3 cells after incubation for 24 h, compared to the untreated group. This suggests that curzerene reduces the migratory ability of HCC cells. Transwell assays were performed to evaluate the invasion rate of cells passing through the Transwell chambers. As observed in Fig. 3C and D, curzerene markedly attenuated the invasion ability of Huh7 and HCCLM3 cells after incubation for 24 h. Gelatinases such as MMP2 and MMP9 have crucial roles in tumor growth and metastasis. We further found reduced MMP2 and MMP9 protein expression in Huh7 and HCCLM3 cells treated with curzerene (Fig. 3E and F).

Curzerene promoted the apoptosis of hepatocellular carcinoma cells

Next, we examined the apoptotic rate of Huh7 and HCCLM3 cells using flow cytometry. Compared to the control cells, curzerene at 20 and 40 μM elevated the apoptotic rate of Huh7 cells to 12.08% and 20.82%, respectively, and elevated the apoptotic rate of

Figure 2. Curzerene induced cell cycle arrest in HCC cells. **A and B:** human HCC cells (Huh7 and HCCLM3) were treated with curzerene for 24 h, followed by measurement of cell proliferation using colony formation experiment. **C and D:** CDK1, cyclin B1 and PCNA protein expression in HCC cells treated with curzerene was measured by immunoblotting. **E and F:** flow cytometry analysis of cell cycle distribution in HCC cells. Measurement data are expressed as mean ± SD. n = 5. *p < 0.05; **p < 0.01; ***p < 0.001.

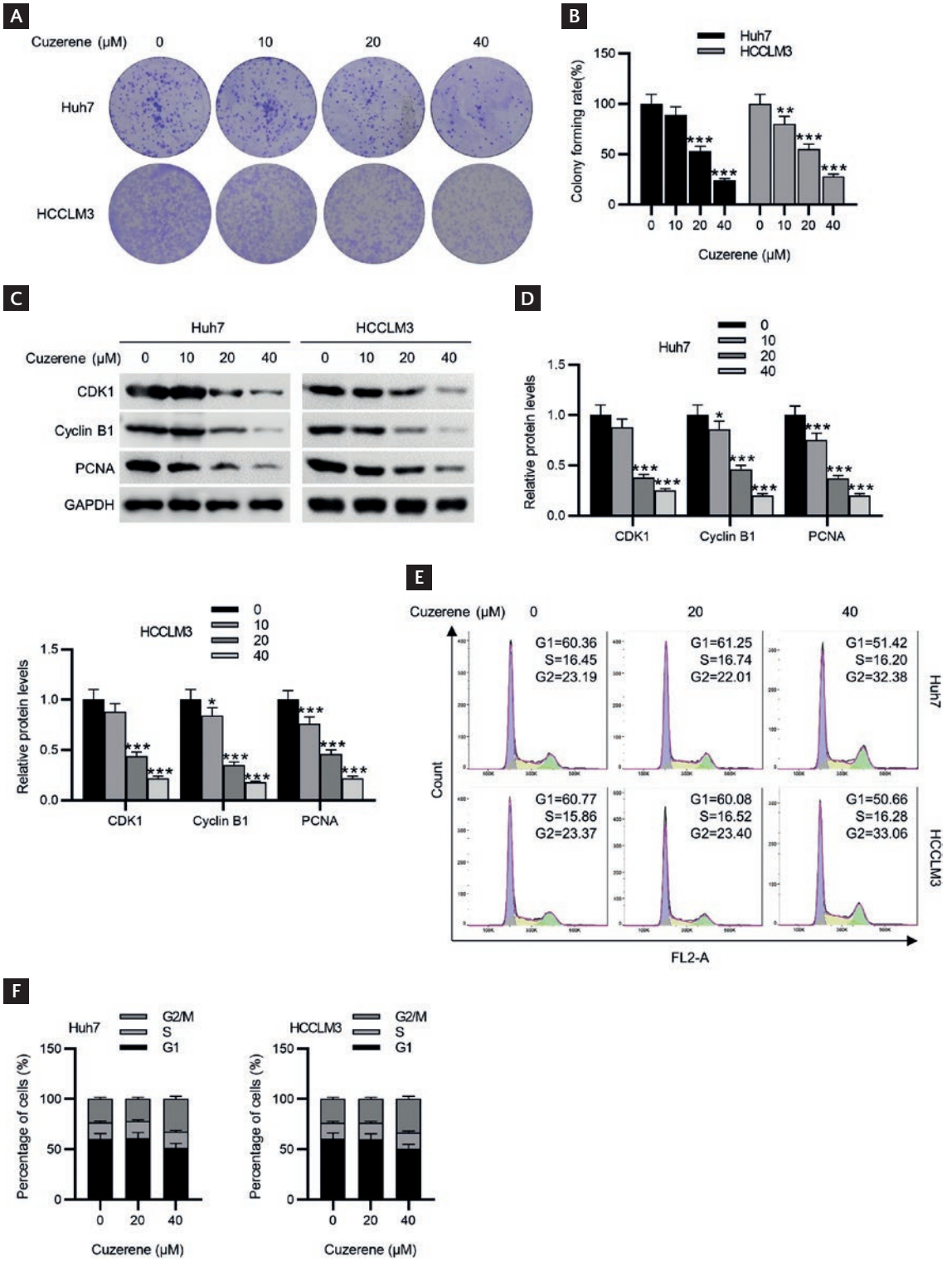

Figure 3. Curzerene suppressed the motility of HCC cells. **A and B:** human HCC cell migration after curzerene treatment was detected by wound healing assay. **C and D:** human HCC cell invasiveness after curzerene treatment was detected by Transwell assay. **E and F:** MMP2 and MMP9 protein expression in HCC cells treated with curzerene was measured by immunoblotting. Measurement data are expressed as mean ± SD. n = 5. **p < 0.01; ***p < 0.001.

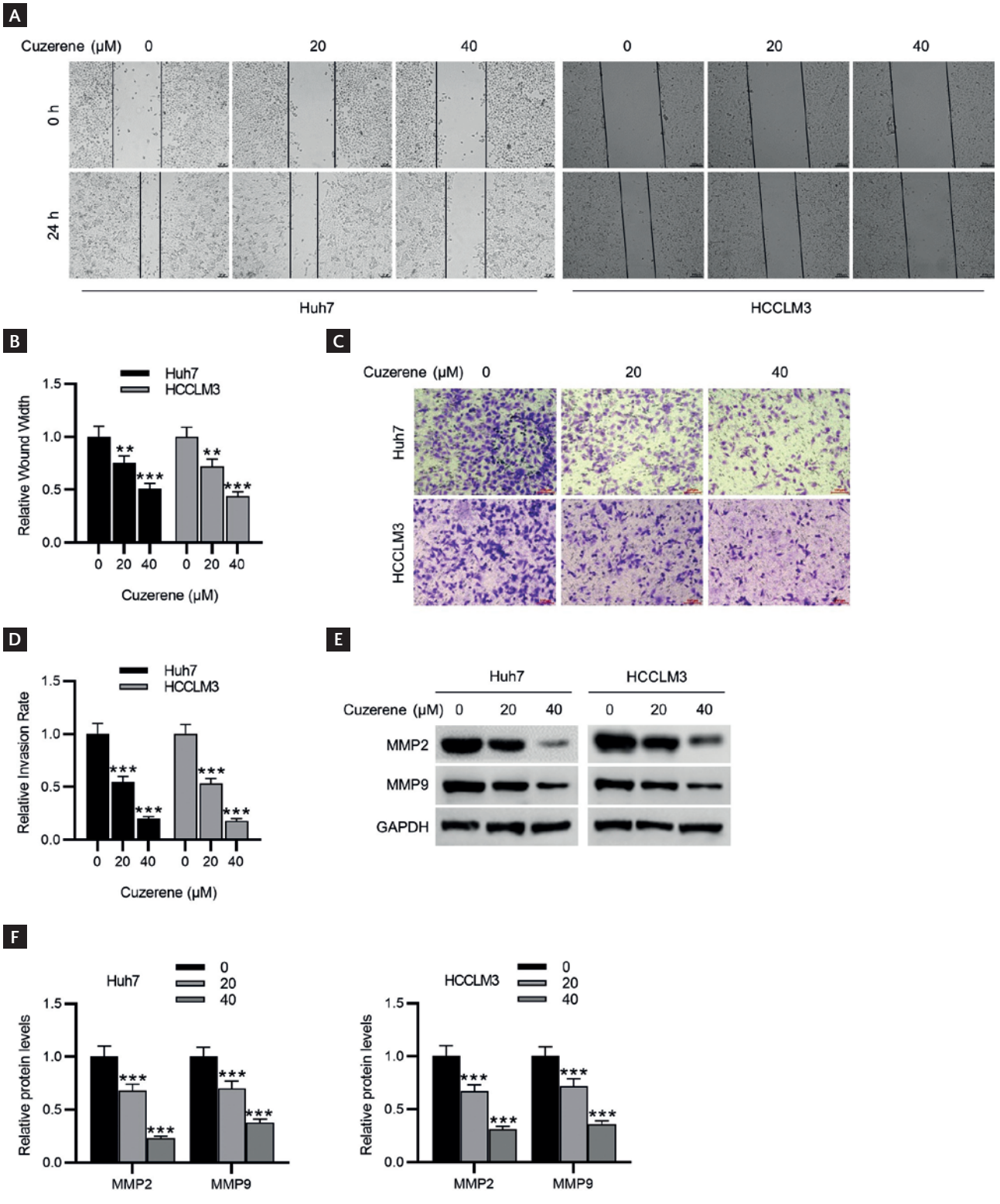

HCCLM3 cells to 12.27% and 21.26%, respectively (Fig. 4A and B). We then examined the expression of apoptotic markers using immunoblotting. The results revealed that both curzerene (20 μM) and curzerene (40 μM) notably upregulated the proapoptotic proteins (Bax, cleaved caspase3, and cleaved PARP) and downregulated the antiapoptotic protein Bcl-2 in Huh7 and HCCLM3 cells (Fig. 4C and D).

Curzerene blocked the PI3K/AKT/mTOR pathway

To investigate the pathways through which curzerene suppresses HCC cell malignancy, the protein levels of the molecules in the PI3K/AKT/mTOR signaling were investigated. Our data showed that curzerene not only restrained the phosphorylation of PI3K but restrained the phosphorylation of PI3K's downstream genes (AKT and mTOR) in Huh7 and HCCLM3 cells (Fig. 5A and B), demonstrating that curzerene might impede HCC progression via the PI3K/AKT/mTOR signaling.

Curzerene repressed tumor growth in a xenograft mouse model

As shown in Fig. 6A-C, curzerene significantly repressed tumor volume and tumor weight when compared to the control group. The curzerene treatment group exhibited reduced expression of CDK1 and cyclin B1 as well as increased expression of Bax, cleaved caspase3, and cleaved PARP (Fig. 6D and E). Immunofluorescence and TUNEL results indicated that curzerene decreased Ki67 expression and increased apoptosis *in vivo* (Fig. 6F-H). Immunofluorescence was used to analyze the expression of p-mTOR in vivo. Consistent with the *in vitro* results, the expression of p-mTOR was significantly reduced in curzerene-treated mice (Fig. 6I).

DISCUSSION

The current investigation reports the anti-tumor efficacy of curzerene in HCC. Our findings revealed that curzerene inhibited the activation of the PI3K/AKT/mTOR pathway, which might mediate the inhibitory effects of curzerene on HCC cell proliferation, invasion, and migration. In addition, curzerene promoted HCC cell apoptosis and induced G2/M cycle arrest. Moreover, we demonstrated that curzerene treatment suppressed HCC tumor growth in xenograft mouse models. These findings demonstrate the potential of curzerene as a novel anti-tumor drug for the treatment of HCC.

Curzerene administration inhibits tumor growth in lung adenocarcinoma cell-bearing nude mice and has no effect on the major organs of the mice, indicating that curzerene has potential for anti-tumor therapy[14]. Notably, curzerene has been shown to repress the progression of glioblastoma via the suppression of glutathione S-transferase A1[13]. Our study showed that curzerene inhibited the viability of HCC cells in a concentration- and time-dependent manner. As a factor in DNA repair and replication machinery, PCNA is essential for nucleic acid metabolism[21]. Ki67 is a nuclear protein associated with cell proliferation[22]. Our data showed that curzerene decreased HCC cell proliferation, as demonstrated by a reduction in PCNA and Ki67 protein expression in curzerene-treated cells and tumors. In addition, the cell cycle is a key target for cancer therapy[23]. Here, we explored whether curzerene can regulate the phase of the cell cycle. Our data revealed that curzerene treatment inhibited the cell cycle at the G2/M phase. Curzerene treatment also decreased the levels of cell cycle-related proteins (CDK1 and cyclin B1). Studies have verified that the highly invasive and migratory capacity of tumors is associated with the high expression of matrix metallopeptidases (MMPs), including MMP2 and MMP9, which are highly expressed in various malignant tumors. They can induce extracellular matrix turnover, thereby promoting tumor migration and invasion[24,25]. Our data showed that the protein expression of MMP2 and MMP9 was markedly reduced in HCC cells treated with curzerene, which might explain the mechanism of how curzerene inhibits cell migration and invasion in HCC.

We evaluated the impact of curzerene on the apoptosis of HCC cells by measuring the levels of apoptosis-related proteins. Cancer cell death acts as a key defense mechanism against cancer progression and is a primary target of cancer therapy[26]. The pro-apoptotic protein Bax disturbs the integrity of the mitochondrial membrane to initiate the process of apoptosis. In contrast, the anti-apoptotic protein Bcl-2 maintains the stability of the mitochondrial membrane to impede apoptosis[27]. Caspase3 plays a key

Figure 4. Curzerene promoted the apoptosis of HCC cells. **A and B:** flow cytometry analysis of cell apoptosis after curzerene treatment. **C and D:** Bcl-2, Bax, cleaved caspase3, and cleaved PARP protein expression in HCC cells after curzerene treatment was measured by immunoblotting. Measurement data are expressed as mean ± SD. n = 5. **p < 0.01; ***p < 0.001.

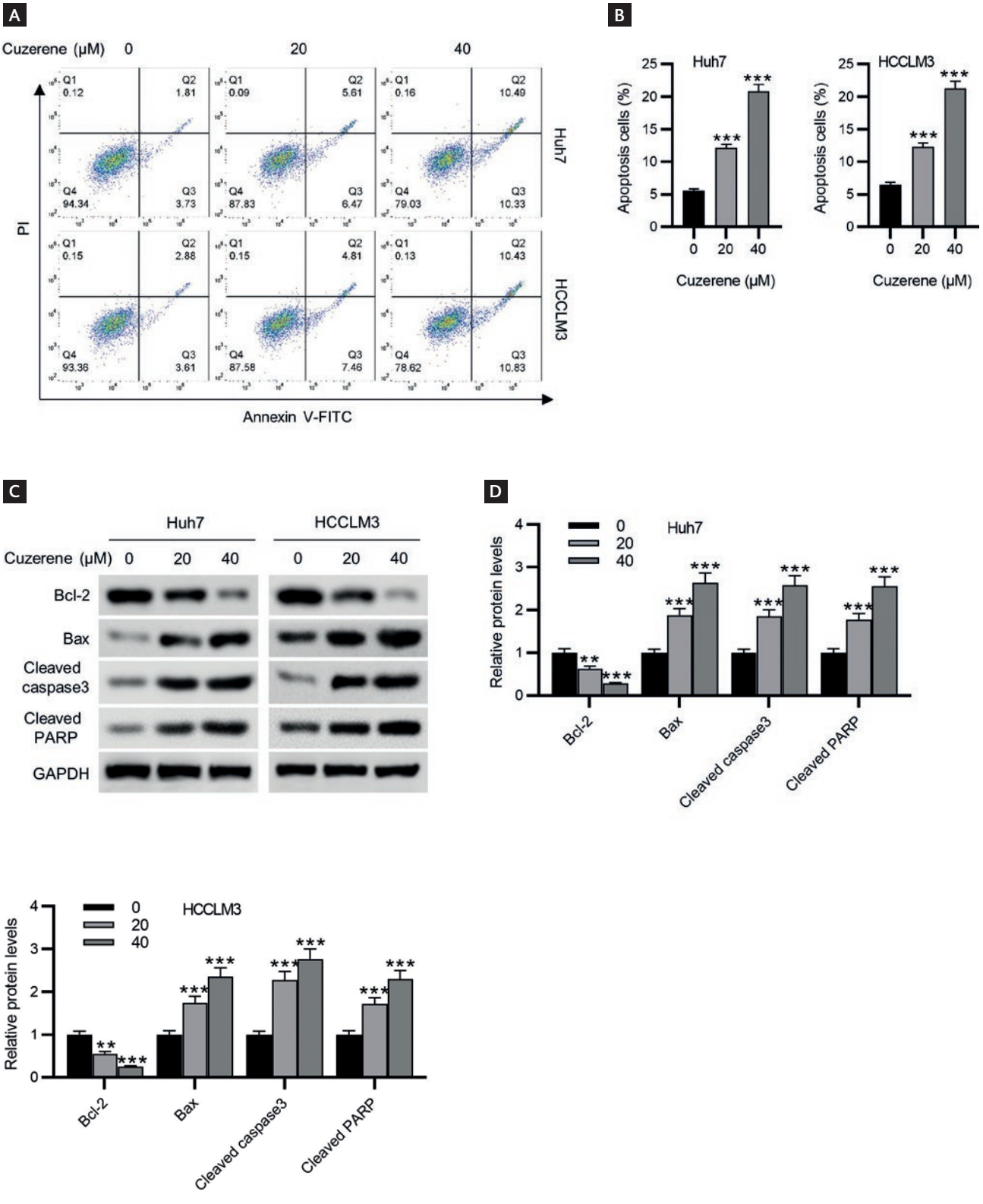

Figure 5. Curzerene blocked the PI3K/AKT/mTOR pathway. **A and B:** immunoblotting analysis of the p-PI3K, PI3K, p-AKT, AKT, mTOR, and p-mTOR protein levels in Huh7 and HCCLM3 cells. Measurement data are expressed as mean ± SD. n = 5. ***p < 0.001.

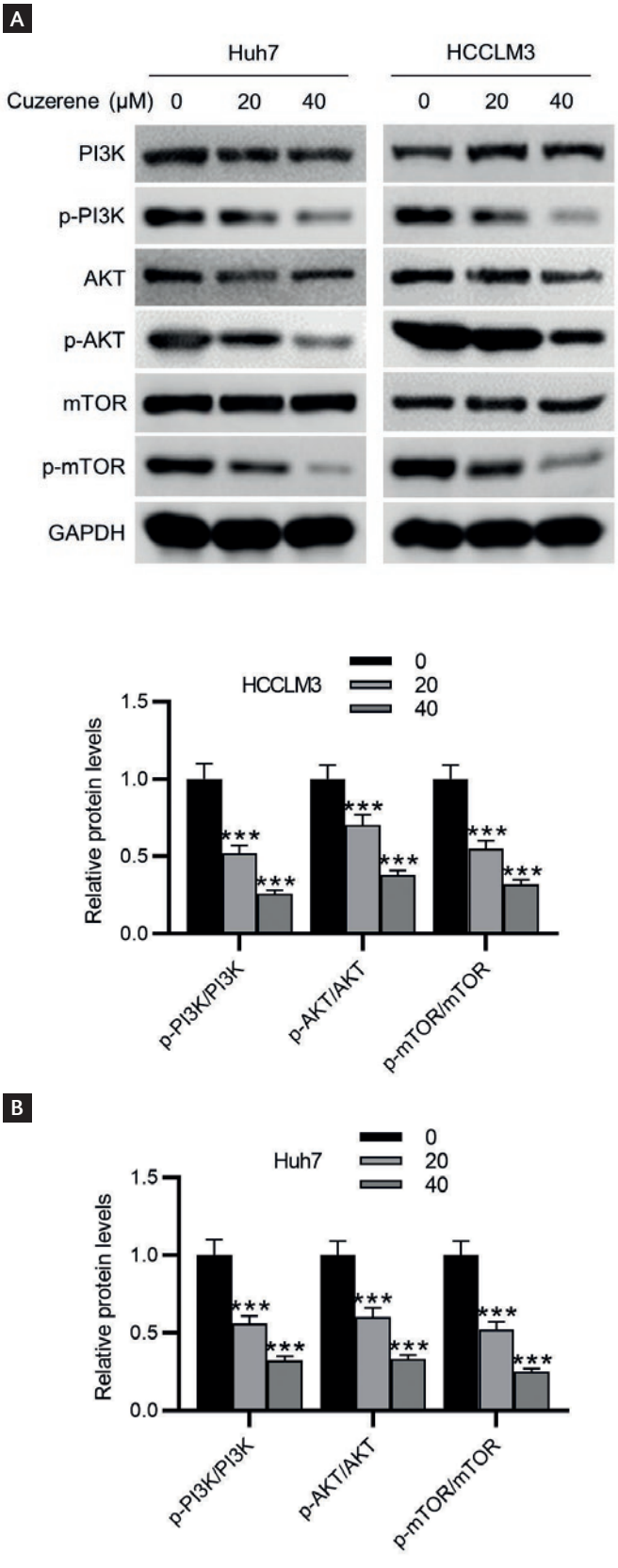

Figure 6. Curzerene inhibited tumor growth in xenograft mouse model. **A:** images of tumors in the control and curzerene groups. **B:** growth curve of tumors in the control and curzerene groups. **C:** tumor weight in the control and curzerene groups. **D and E:** immunoblotting analysis of the CDK1, cyclin B1, Bax, cleaved caspase3, and cleaved PARP protein levels in the tumors. **F:** immunofluorescence analysis of Ki67 and TUNEL staining in the tumors. **G:** quantification of Ki67-positive cells. **H:** Quantification of TUNEL staining. **I:** immunofluorescence was used to detect the expression of p-mTOR in the tumors. **J:** proposed mechanism of how curzerene inhibits HCC via the PI3K/AKT/mTOR cascade. Measurement data are expressed as the mean ± SD. n = 4. **p < 0.01; ***p < 0.001.

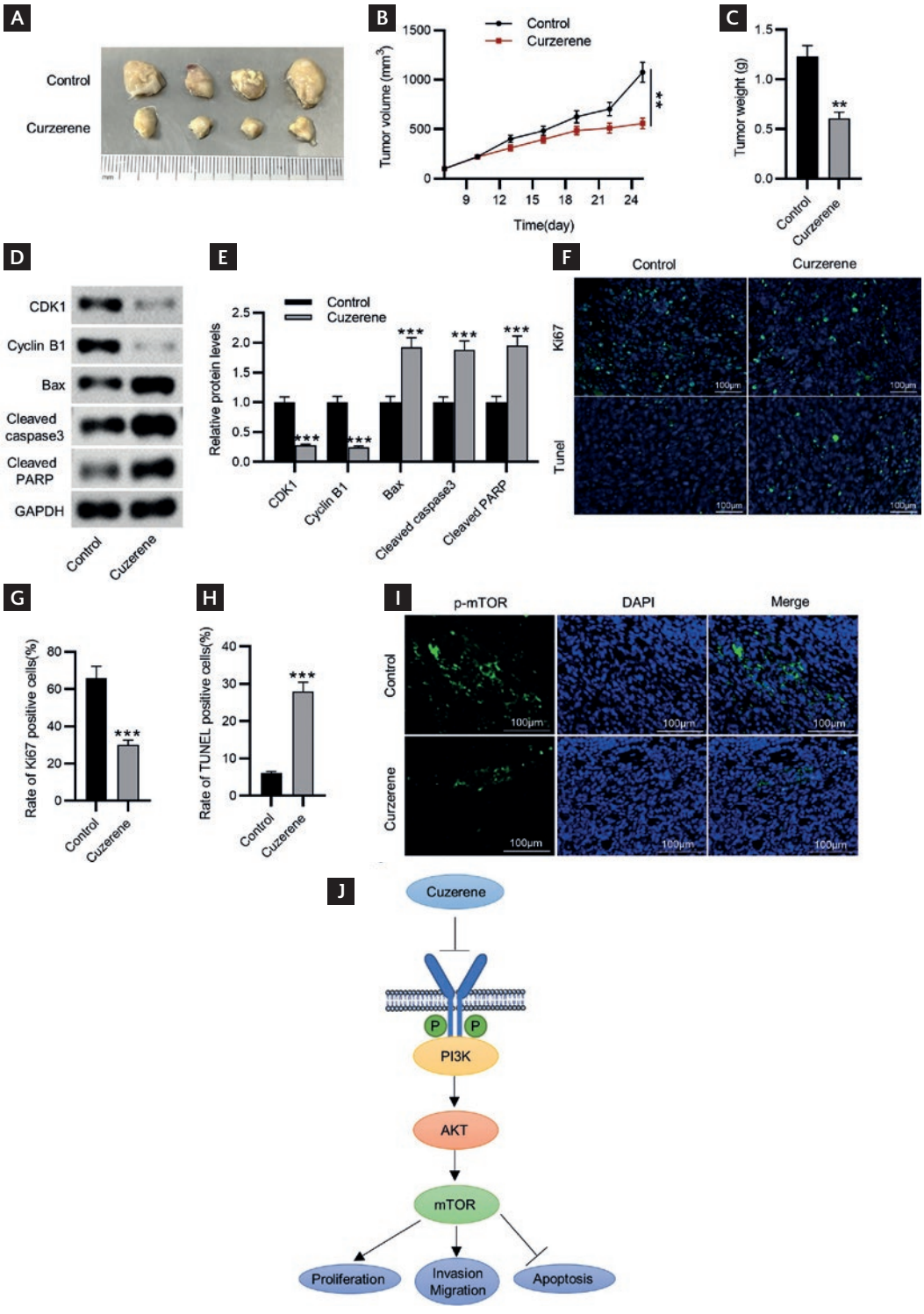

role in apoptosis by triggering the activation of endonuclease Caspase-activated DNAse, leading to the degradation of chromosomal DNA[28]. PARP is a key protein involved in DNA repair. The PARP protein is cleaved during apoptosis, suggesting a role for PARP in DNA damage-induced cell death[29]. In this study, we found that curzerene notably inhibited the upregulation of Bax and the activation of cleaved caspase3 and cleaved PARP in HCC cells. Simultaneously, curzerene induced a reduction in the expression levels of the antiapoptotic protein Bcl-2. These data demonstrate the apoptosis-promoting role of curzerene in HCC.

PI3K/AKT/mTOR signaling is a crucial pathway that contributes to cell proliferation and inhibits cell apoptosis in HCC, and activation of this pathway facilitates the malignant progression of cancer[30,31]. The mTOR signaling inhibitors exhibit prominent antiproliferative effects in both *in vitro* and *in vivo* models. However, these inhibitors are toxic to patients with chronic liver disease[32]. Previous studies have revealed that curzerene is an effective and safe therapeutic agent[14]. Here, we found that curzerene restrained the activation of the PI3K/AKT/mTOR pathway in HCC cells, suggesting that curzerene hinders HCC progression via the inhibition of the PI3K/AKT/mTOR pathway. We also demonstrated that curzerene inhibited tumor growth *in vivo* by inhibiting proliferation and promoting apoptosis through the suppression of mTOR.

Overall, we demonstrate that curzerene restrains the proliferation and facilitates the apoptosis of HCC cells. Moreover, curzerene inhibited the growth of xenografted HCC cells *in vivo*. The anti-tumor efficacy of curzerene may be mediated by the inactivation of the PI3K/AKT/mTOR pathway (Fig. 6J). Our investigation may provide new insights into the anti-tumor potential of curzerene in HCC.

ACKNOWLEDGMENTS

The work was supported by the National Natural Science Foundation of China (Grant No. 81960910), the Guangxi Science and Technology Base and Talent Project (Grant No.AD18281094), and the Guangxi International Zhuang Medicine Hospital "Green Seedling Project" Talent Cultivation Project. All experimental procedures were approved by the Institutional Animal Care and Use Committee of Guangxi International Zhuang Medicine Hospital.

SUPPLEMENTARY MATERIAL

The datasets generated during and/or analyzed during the current study are available from the corresponding author on reasonable request.

REFERENCES

1. Sung H, Ferlay J, Siegel RL, Laversanne M, Soerjomataram I, Jemal A, et al. Global Cancer Statistics 2020: GLOBOCAN estimates of incidence and mortality worldwide for 36 cancers in 185 countries. CA Cancer J Clin. 2021;71:209-49.
2. Ferlay J, Colombet M, Soerjomataram I, Dyba T, Randi G, Bettio M, et al. Cancer incidence and mortality patterns in Europe: estimates for 40 countries and 25 major cancers in 2018. Eur J Cancer. 2018;103:356-87.
3. Wen Q, Chan KH, Shi K, Lv J, Guo Y, Pei P, et al. Tobacco smoking and solid fuels for cooking and risk of liver cancer: a prospective cohort study of 0.5 million Chinese adults. Int J Cancer. 2022;151:181-90.
4. He F, Sha Y, Wang B. Relationship between alcohol consumption and the risks of liver cancer, esophageal cancer, and gastric cancer in China: meta-analysis based on case-control studies. Medicine (Baltimore). 2021;100:e26982.
5. Kimanya ME, Routledge MN, Mpolya E, Ezekiel CN, Shirima CP, Gong YY. Estimating the risk of aflatoxin-induced liver cancer in Tanzania based on biomarker data. PLoS One. 2021;16:e0247281.
6. Rizzo GE, Cabibbo G, Craxì A. Hepatitis B virus-associated hepatocellular carcinoma. Viruses. 2022;14:986.
7. Maluccio M, Covey A. Recent progress in understanding, diagnosing, and treating hepatocellular carcinoma. CA Cancer J Clin. 2012;62:394-9.
8. Zhu Q, Qiao G, Xu C, Yu X, Zhao J, Yu Z, et al. Conditional survival in patients with spontaneous tumor rupture of hepatocellular carcinoma after partial hepatectomy: a propensity score matching analysis. HPB (Oxford). 2019;21:722-30.
9. Cheng Z, Yang P, Qu S, Zhou J, Yang J, Yang X, et al. Risk factors and management for early and late intrahepatic recurrence of solitary hepatocellular carcinoma after curative resection. HPB (Oxford). 2015;17:422-7.
10. Ikeda M, Morizane C, Ueno M, Okusaka T, Ishii H, Furuse J. Chemotherapy for hepatocellular carcinoma: current status and future perspectives. Jpn J Clin Oncol. 2018;48:103-14.
11. Jeong SJ, Koh W, Kim B, Kim SH. Are there new therapeutic options for treating lung cancer based on herbal medicines and their metabolites? J Ethnopharmacol. 2011;138:652-61.
12. Salehi B, Stojanović-Radić Z, Matejić J, Sharifi-Rad M, Anil Kumar NV, Martins N, et al. The therapeutic potential of curcumin: a review of clinical trials. Eur J Med Chem. 2019;163:527-45.
13. Cheng B, Hong X, Wang L, Cao Y, Qin D, Zhou H, et al. Curzerene suppresses progression of human glioblastoma through inhibition of glutathione S-transferase A4. CNS Neurosci Ther. 2022;28:690-702.
14. Wang Y, Li J, Guo J, Wang Q, Zhu S, Gao S, et al. Cytotoxic and antitumor effects of curzerene from Curcuma longa. Planta Med. 2017;83:23-9.
15. Pópulo H, Lopes JM, Soares P. The mTOR signalling pathway in human cancer. Int J Mol Sci. 2012;13:1886-918.
16. Mossmann D, Park S, Hall MN. mTOR signalling and cellular metabolism are mutual determinants in cancer. Nat Rev Cancer. 2018;18:744-57.

17. Liu X, Xiao M, Zhang L, Li L, Zhu G, Shen E, et al. The m6A methyltransferase METTL14 inhibits the proliferation, migration, and invasion of gastric cancer by regulating the PI3K/AKT/mTOR signaling pathway. J Clin Lab Anal. 2021; 35:e23655.
18. Chen K, Zhu P, Chen W, Luo K, Shi XJ, Zhai W. Melatonin inhibits proliferation, migration, and invasion by inducing ROS-mediated apoptosis via suppression of the PI3K/Akt/mTOR signaling pathway in gallbladder cancer cells. Aging (Albany NY). 2021;13: 22502-15.
19. American Diabetes Association. Gestational diabetes mellitus. Diabetes Care. 2004;27 Suppl 1:S88-90.
20. Chen S, Yan W, Lang W, Yu J, Xu L, Xu X, et al. SESN2 correlates with advantageous prognosis in hepatocellular carcinoma. Diagn Pathol. 2017;12:13.
21. Pal HC, Katiyar SK. Cryptolepine, a plant alkaloid, inhibits the growth of non-melanoma skin cancer cells through inhibition of topoisomerase and induction of DNA damage. Molecules. 2016; 21:1758.
22. Bologna-Molina R, Mosqueda-Taylor A, Molina-Frechero N, Mori-Estevez AD, Sánchez-Acuña G. Comparison of the value of PCNA and Ki-67 as markers of cell proliferation in ameloblastic tumors. Med Oral Patol Oral Cir Bucal. 2013;18: e174-9.
23. Jamasbi E, Hamelian M, Hossain MA, Varmira K. The cell cycle, cancer development and therapy. Mol Biol Rep. 2022;49: 10875-83.
24. Zhang C, Wang L, Chen J, Liang J, Xu Y, Li Z, et al. Knockdown of Diaph1 expression inhibits migration and decreases the expression of MMP2 and MMP9 in human glioma cells. Biomed Pharmacother. 2017;96:596-602.
25. Zhang JF, Wang P, Yan YJ, Li Y, Guan MW, Yu JJ, et al. IL 33 enhances glioma cell migration and invasion by upregulation of MMP2 and MMP9 via the ST2-NF-κB pathway. Oncol Rep. 2017; 38:2033-42.
26. Tang H, Zhang Y, Li D, Fu S, Tang M, Wan L, et al. Discovery and synthesis of novel magnolol derivatives with potent anticancer activity in non-small cell lung cancer. Eur J Med Chem. 2018; 156:190-205.
27. Baig S, Seevasant I, Mohamad J, Mukheem A, Huri HZ, Kamarul T. Potential of apoptotic pathway-targeted cancer therapeutic research: where do we stand? Cell Death Dis. 2016;7:e2058.
28. Jan R, Chaudhry GE. understanding apoptosis and apoptotic pathways targeted cancer therapeutics. Adv Pharm Bull. 2019; 9:205-18.
29. Müller V, Wöckel A, Lux MP, Janni W, Hartkopf AD, Nabieva N, et al. Update breast cancer 2018 (Part 4) - genomics, individualized medicine and immune therapies - in the middle of a new era: treatment strategies for advanced breast cancer. Geburtshilfe Frauenheilkd. 2018;78:1119-28.
30. Li Z, Li Y, Jia Y, Ding B, Yu J. Rab1A knockdown represses proliferation and promotes apoptosis in gastric cancer cells by inhibition of mTOR/p70S6K pathway. Arch Biochem Biophys. 2020; 685:108352.
31. Sun EJ, Wankell M, Palamuthusingam P, McFarlane C, Hebbard L. Targeting the PI3K/Akt/mTOR pathway in hepatocellular carcinoma. Biomedicines. 2021;9:1639.
32. Ferrín G, Guerrero M, Amado V, Rodríguez-Perálvarez M, De la Mata M. Activation of mTOR signaling pathway in hepatocellular carcinoma. Int J Mol Sci. 2020;21:1266.